FOR THE RECORD

Combining different design strategies for rational affinity maturation of the MICA-NKG2D interface

Samuel H. Henager, Melissa A. Hale, Nicholas J. Maurice, Erin C. Dunnington, Carter J. Swanson, Megan J. Peterson, Joseph J. Ban, David J. Culpepper, Luke D. Davies, Lisa K. Sanders, and Benjamin J. McFarland*

Department of Chemistry and Biochemistry, Seattle Pacific University, Seattle, Washington 98119-1997

Received 15 February 2012; Revised 19 June 2012; Accepted 21 June 2012
DOI: 10.1002/pro.2115
Published online 3 July 2012 proteinscience.org

Abstract: We redesigned residues on the surface of MICA, a protein that binds the homodimeric immunoreceptor NKG2D, to increase binding affinity with a series of rational, incremental changes. A fixed-backbone RosettaDesign protocol scored a set of initial mutations, which we tested by surface plasmon resonance for thermodynamics and kinetics of NKG2D binding, both singly and in combination. We combined the best four mutations at the surface with three affinity-enhancing mutations below the binding interface found with a previous design strategy. After curating design scores with three cross-validated tests, we found a linear relationship between free energy of binding and design score, and to a lesser extent, enthalpy and design score. Multiple mutants bound with substantial subadditivity, but in at least one case full additivity was observed when combining distant mutations. Altogether, combining the best mutations from the two strategies

Additional Supporting Information may be found in the online version of this article.

Author contributions: S.H.H. designed and completed protein biochemistry and computational experiments and edited the manuscript; M.A.H., N.J.M., E.C.D., C.J.S., M.J.P., J.J.B., L.D.D., and L.K.S. designed and completed DNA mutagenesis, protein expression, purification, assessment, and data analysis and edited the manuscript; D.J.C. designed and completed computational experiments and edited the manuscript; and B.J.M.: conceived and designed the experiments, completed computational experiments, and wrote the manuscript.

Carter J. Swanson's current address is the Department of Biophysics, University of Michigan, Ann Arbor, MI 48109.
Megan J. Peterson's current address is the Institute of Molecular Biology, University of Oregon, Eugene, OR 97403.
Lisa K. Sanders's current address is the School of Medicine, University of Washington, Seattle, WA 98195.

Grant sponsor: NIH; Grant number: 2 R15 AI058972-02 (to B.J.M.); Grant sponsor: Seattle Pacific University Montana Endowment Grant (to B.J.M.).

Correspondence to: Benjamin McFarland, Seattle Pacific University, Suite 205, 3307 Third Avenue West, Seattle, WA 98119-1997. E-mail: bjm@spu.edu

into a septuple mutant enhanced affinity by 50-fold, to 50 nM, demonstrating a simple, effective protocol for affinity enhancement.

Keywords: protein design; protein–protein interaction; immunoreceptors; additivity; free energy of binding; thermodynamics and kinetics of binding; van't Hoff enthalpy

Introduction

Improvement of protein–protein binding has utility in applications ranging from *in vitro* assays to *in vivo* therapies.[1] Different strategies for enhancing affinity incorporate combinatorial and/or computational design: combinatorial design tests large populations of randomized mutants in a process similar to antibody affinity maturation, whereas computational or rational design calculates the biochemical stability of protein conformations and amino acid mutations using various scoring functions.[2] Computational optimization of the chemical interactions in proteins has successfully stabilized protein–protein interfaces with final K_D values ranging from micromolar to picomolar (Supporting Information Table S1), although substantial challenges remain.[3–5] Computational and combinatorial techniques can work together, as when computational techniques created a *de novo* 200 nM interface between influenza hemagglutinin and a binding scaffold, and then affinity maturation via combinatorial screening produced three mutations that together brought the affinity to 4 nM.[6]

Previously, we used the rational design algorithm RosettaDesign to enhance the affinity of the interface between the immunoproteins NKG2D and MICA.[7] This interaction acts as a dominant activating trigger for NK cells and is involved in several pathologies.[8] Our first design strategy targeted residues that do not directly contact NKG2D to alter the stability of unbound MICA and affect NKG2D binding indirectly [Fig. 1(A)].[7] Extrainterfacial changes

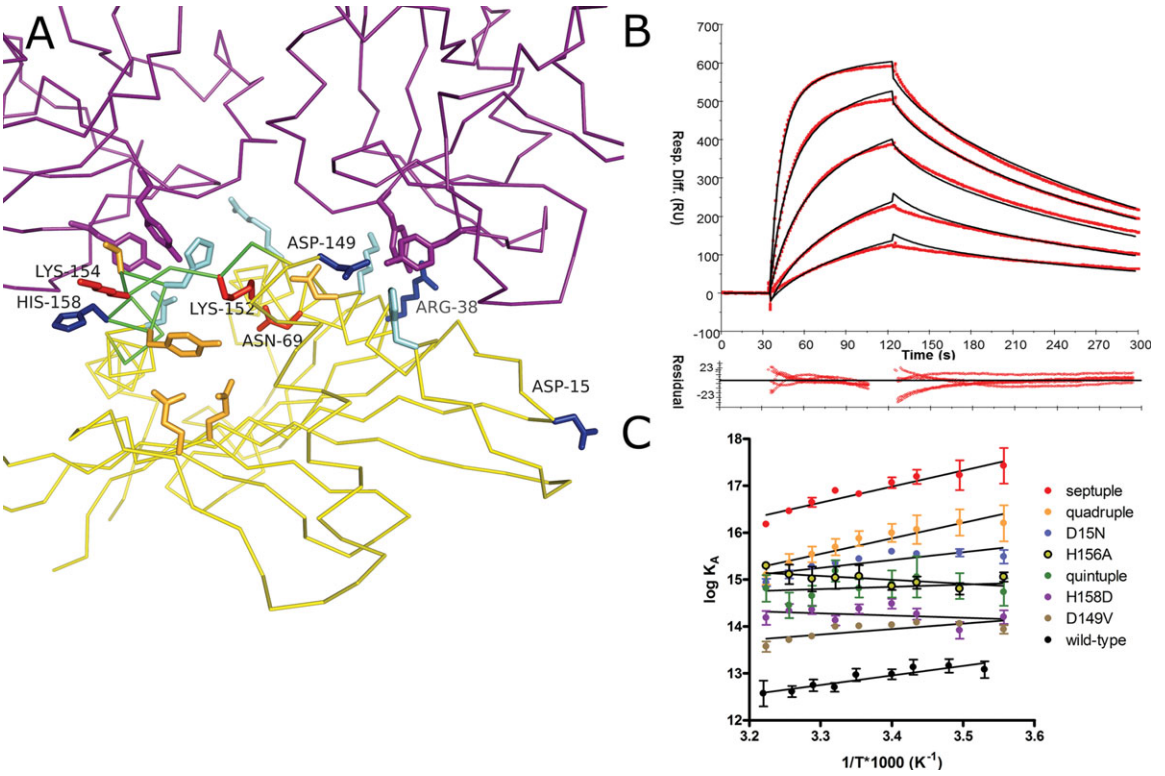

Figure 1. Locations redesigned with two strategies and measurement of binding thermodynamics and kinetics. (A) Targets for design highlighted in the structure for the NKG2D-MICA complex (purple: NKG2D homodimer with core tyrosines shown as sticks; yellow: MICA with redesigned residues shown as sticks; green: backbone of "disordered loop" region of MICA that is not observed in the unbound MICA structure; orange/red: subinterfacial residues redesigned in first strategy, with stabilizing residues combined in septuple mutant in red and labeled; light blue/dark blue: interfacial residues redesigned in second strategy, with stabilizing residues combined in septuple mutant in dark blue and labeled). Figure was made using Pymol http://www.pymol.org/. (B) SPR sensorgrams and residuals for injection of serial dilutions of NKG2D over a MICA-coupled dextran surface (red: kinetic data collected; black: two-step model fit). (C) van't Hoff plots of four single and three multiple mutants for triplicate SPR data at nine temperatures, with K_A values calculated from kinetic data and enthalpies of binding calculated from linear slopes as described in Lengyel *et al*.

in MICA that enhanced affinity for NKG2D were predicted to destabilize the region underneath the interface. A triple mutant was found with this strategy that bound with 17-fold enhanced affinity.

Because none of these mutations directly contacts NKG2D, we began a second round of rational design in which MICA residues that directly contact NKG2D were optimized with RosettaDesign to enhance interfacial affinity, with the goal of combining the mutations from the two strategies. Single mutations predicted to enhance affinity were expressed, purified, and tested experimentally. Then mutations were combined iteratively with other surface mutations, and with the most affinity-enhancing mutations from our first subinterfacial design strategy, to investigate the cumulative effect of designed mutations at a protein–protein interface.

Results and Discussion

RosettaDesign[9] calculated an optimal amino acid (selecting any amino acid except cysteine) 100 times for each of the 22 MICA residues that contact NKG2D in the MICA-NKG2D complex structure (PDB ID: 1HYR).[10] Each location was varied individually and all other residues were wild-type. For 11 locations, Rosetta either returned the wild-type residue or a similar residue with insignificant predicted stabilization (score >-0.05), and the other 11 mutations were investigated through experiment (bold type in Supporting Information Table S2). Also, calculations were done in which all MICA contact residues were allowed to vary at once. In the set of 100 such calculations, alterative stabilizing residues were chosen by the algorithm more than 10% of the time at six locations, which were added to the experimental set as single mutants (normal type in Supporting Information Table S2). These 17 single mutants were produced by site-directed mutagenesis, expressed in *Escherichia coli* as inclusion bodies, then refolded and purified by affinity and size-exclusion chromatography. Each MICA mutant was amine-coupled to a dextran surface on a gold chip and its affinity for NKG2D measured by surface plasmon resonance (SPR) [Fig. 1(B) and Supporting Information Table S2]. For 11 mutants binding with affinities similar to or stronger than wild-type, affinities were determined at nine temperatures and van't Hoff plots constructed to calculate enthalpies of binding [Fig. 1(C)]. Overall, this simple design technique produced seven mutants that stabilized the interaction with NKG2D by 0.5 kcal/mol or more, with two stabilized by more than 1.0 kcal/mol [Fig. 2(A)].

The best single mutations at the interface were combined in 18 multiple-mutant MICA molecules, which were analyzed for NKG2D binding by SPR (Supporting Information Table S2). Most of the single mutants stabilized the interaction with NKG2D significantly, but combining mutations at the interface resulted in eight MICA molecules stabilized by 0.5 kcal/mol or more, four of which were stabilized by more than 1.0 kcal/mol [Fig. 2(A)]. The best multiple mutant from this step of the strategy combined four of the best five single mutations, increasing affinity by -1.74 kcal/mol about half of a kcal/mol better than the best single mutant. The H156A mutation was excluded from this combination after we observed that, despite its highly stabilizing character in the context of wild-type MICA, this mutation produced negative additivity when combined with other mutations suggested by RosettaDesign in several multiple mutants [Fig. 2(B)]. H156A fails the first of our three design tests below because Rosetta predicts an unrealistically large upper-quintile stabilization to both bound and unbound proteins. Inspection of the predicted structural model for H156A reveals that His156 forms few specific interactions with NKG2D, and when it is mutated to an alanine, a cavity is created in the center of the disordered loop region of MICA that may allow other mutations to shift in a manner not captured by our fixed-backbone assumptions and/or may increase stability and reduce flexibility of this region in which flexibility is important to binding.[7] Removing this mutation from the quintuple mutant resulted in a 0.65 kcal/mol stabilization of interaction with NKG2D.

In the final step of design, we combined the best three subinterfacial mutations found previously[7] with the four best interfacial mutations. The resulting mutant bound NKG2D with a 50-fold enhanced affinity, which is a -2.29 kcal/mol stabilization relative to wild-type at 25°C [Fig. 2(A)]. This is similar to many computational results (Supporting Information Table S1), but it is also partially subadditive by about a kcal/mol relative to the added affinities of the triple and quadruple mutants from the two design strategies [Fig. 2(B)]. The affinity enhancement of the septuple mutant was confirmed with a previously developed size-exclusion chromatography assay[11] in which the mutant was mixed with NKG2D and injected at a slow flow rate. Under these conditions, the septuple mutant eluted as a large peak ($\sim$60 kDa), indicating that the complex had persisted through the column, but wild-type MICA eluted as a small peak ($\sim$30kDa) corresponding to unbound MICA monomer and NKG2D dimer.

Design scores were calculated with RosettaDesign for all expressed mutants to compare fixed-backbone design calculations with experimental results (Supporting Information Table S3). We calibrated and cross-validated our NKG2D-MICA calculations with 44 designed models recapitulating published binding data for mutations at two

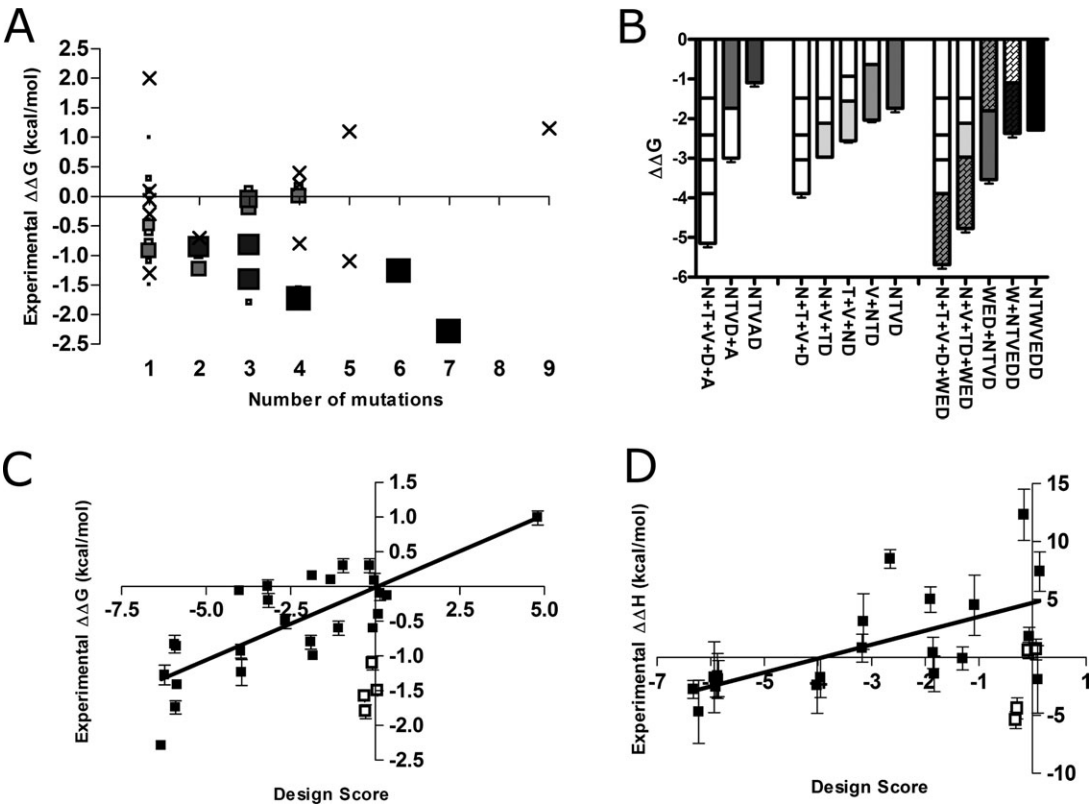

Figure 2. Comparison of design scores (=bound complex score–unbound MICA score relative to wild-type scores) to binding thermodynamics of single and multiple mutants relative to wild-type MICA. (A) Experimentally determined free energies of binding for all mutants tested arranged by number of mutations made (□: passed all three tests and sized and shaded by relative design score, with best design score largest and colored black; X: failed one of the three design score tests). (B) Additivity of mutants arranged with three sets of examples: negative additivity of H156A, subadditivity of D15N, and both subadditivity and full additivity of N69W Bars shaded by number of mutations, from white:one mutation to black:seven mutations; patterned bars:subinterfacial mutations from the first strategy. N = D15N; T = R38T; V = D149V; D = H158D; A = H156A . Third section only: W = N69W; E = K152E; second D = K154D. (C) Relationship between experimentally determined free energy of binding and design score and (D) between enthalpy of binding and design score for mutants shown as black boxes that pass the three tests (□: first-strategy N69W and second-strategy D15N mutants discussed in the text and closely related combined mutants WED and NWED). R^2 values for linear regression fits = 0.61 and 0.40, respectively.

antibody-antigen interfaces[12] and a TCR-MHC interface[13], with affinities ranging from picomolar to micromolar (Supporting Information Table S4). Some design scores were apparent outliers by about an order of magnitude, either from steric clashes producing high repulsive energies or from unrealistic stabilization calculations for particular interactions. Three tests separated out the most extreme upper-quintile calculated results:

1 *Is the change the total design score undergoes upon mutation within the 80th percentile of all total scores?* This was calculated as the absolute value of any of the following relative to wild-type: unbound ligand alone, bound protein–protein complex, or the subtracted value of unbound-bound [Eq. (1)]. For our set of NKG2D-MICA scores, this corresponded to a value less than about ±20 (Supporting Information Fig. S1). In terms of Table S2, a passing score means the following equation was true for the columns titled unbound, bound, and bound-unbound (which is the unbound value subtracted from the bound value to calculate the change in energy upon binding):

$$|\text{Total design score}| < 20 \quad (1)$$

2 *Is the change the total design score undergoes on mutation within the 80th percentile of all of Rosetta's repulsive term (fa_rep) scores?* For our set of NKG2D-MICA scores, this also corresponded to a value less than about ±20. In terms of the columns in Table S3, a passing score means the following equation was true for the columns Δrep_MICA (unbound), Δrep_complex (bound), and the two columns subtracted (as Δrep_complex − Δrep_MICA):

$$|\text{fa\_rep for mutant} - \text{fa\_rep for wild-type}| < 20 \quad (2)$$

These two tests are similar to the criterion that the design should not be predicted to significantly

destabilize the unbound molecules,[14] also excluding unusually large predicted stabilization. Eight designs of the 41 NKG2D-MICA mutants failed one or both of the first two tests.

3 *For the subtracted value of bound-unbound only: does Rosetta's side chain hydrogen bonding term (hb_sc) stay the same or decrease?* This threshold was suggested by Sammond *et al*. to counteract Rosetta's reported tendency to replace a good hydrogen bond with a less specific — for example, hydrophobic — interaction in the bound complex,[14] and corresponds to the 80th percentile of our set of hb_sc scores. We follow Sammond *et al*. in using the subtracted value only (=bound–unbound), to the first decimal place, so that a score of less than 0.05 is considered to stay the same within error. In terms of the columns in Table S3, the Δhb_sc_MICA value was subtracted from the Δhb_sc_complex value so that a passing score means the following equation was true:

$$[(\text{hb\_sc for mutant complex} - \text{hb\_sc wild-type complex}) - (\text{hb\_sc for mutant MICA} - \text{hb\_sc for wild-type MICA})] < 0.05 \quad (3)$$

Four more NKG2D-MICA designs failed this test.

Application of these thresholds to other interfaces could use either the percentile or the raw score depending on the number of scores in the design set. Cross-validation with the experimental binding data published for 44 mutations at the three other interfaces showed that the three tests marked out 20 of Rosetta's scores for these mutations as suspect, 17 of which were successful applications of the tests (either incorrect predictions by Rosetta or correct predictions of destabilization; Supporting Information Fig. S2). Interestingly, all three cases in which the tests did not succeed—experimentally stabilizing mutants correctly predicted by Rosetta yet incorrectly excluded by the tests—replaced glycine residues: two of these predicted the effects of mutating glycines in the low-affinity MHC-TCR complex and the third altered a glycine in an antibody CDR loop. The MHC-TCR complex produced the most incorrect predictions by Rosetta. For example, several TCR mutants that replace a smaller residue with a larger one fail tests 1 and 2 because of steric repulsion in the complex (D26W and G28L) or in the unbound TCR (G28I). *In silico*, the fixed-backbone model cannot avoid these repulsions, but *in vitro*, these mutants improve binding; in these cases, small backbone movements would minimize repulsion. Rosetta scores for two other TCR mutations (G28M and S100T) passed all three tests, yet incorrectly predicted destabilization of the complex; in these cases, loop adjustments may allow stabilizing interactions to form in the complex by the new side chain atoms that cannot be reached in our fixed-backbone models. In general, Rosetta was able to more accurately estimate quantitative effects of mutation for the higher-affinity antibody-antigen complexes, but in all three cases, the tests would have pre-filtered the predictions so that a more experimentally amenable set of stabilizing mutations remained.

After these tests were applied to curate the Rosetta data for NKG2D-MICA, correlations were observed for the remaining data, using the subtracted design score suggested by Sammond *et al*.[14] The best design score corresponds to the best experimental result, which is the septuple mutant [Fig. 2(A)]. A linear relationship is observed between the change in free energy of binding as determined by SPR and the design score [Fig. 2(C)], and a similar but more dispersed relationship is observed between van't Hoff enthalpy of binding and design score (note that enthalpy measurements have a larger standard error as well) [Fig. 2(D)]. Linear relationships within some error have been observed between free energy of binding and design score for various design methods.[12,15,16] The linear relationship shown here between enthalpy of binding and Rosetta's design score suggests that fixed-backbone Rosetta calculations better recapitulate characteristics associated with enthalpy (e.g., charge-charge interactions, close atom packing) than with entropy (e.g., flexibility).

Each design strategy produced one significantly stabilizing ($\Delta\Delta G < -0.5$ kcal/mol), peripherally located mutation that Rosetta does not predict as stabilizing: N69W for the subinterfacial strategy and D15N for the interfacial strategy. These may promote NKG2D-MICA interface formation through mechanisms more complex than optimizing direct atomic contacts. For example, N69W is predicted to destabilize the unbound MICA molecule, which biophysical tests have confirmed,[7] and which is reflected in the positive total design score for unbound MICA relative to wild-type. In MHC molecules, which are structurally homologous to MICA, flexibility of the helices in the center of the binding surface influences T-cell receptor binding.[17,18] Such movements in MICA would not be captured by fixed-backbone calculations. D15N alters charge distribution on the outer edge of the interface, and is predicted to stabilize the MICA-NKG2D complex, but also to stabilize the unbound MICA by the same amount so that the subtracted design score prediction is close to zero. Empirically, we found that this mutation, alone and in combination with other mutants, successfully stabilizes the interface.

Combining mutations at an interface can result in different degrees of additivity,[19,20,15] with subadditivity observed for a T-cell receptor-MHC interface[21] and a single-chain Fv-PSA interface.[22] Similarly, we repeatedly observed subadditivity and negative additivity at this interface [Fig. 2(B)]. In a

study of antibody affinity maturation, interface affinity was found to be inherently limited,[23] so the NKG2D-MICA interface architecture may impose a structural limit here, particularly the requirement that a homodimer engage a monomer with two symmetric half-sites on a flat surface. Also, mutations located in independent modules distant from each other combine additively,[19,20] and the arrangement of each NKG2D half-site as residues clustered around a pair of tyrosines may cause each half-site to cooperate as a single non-additive module. When the NKG2D-MICA crystal structure was analyzed for modules according to the technique of Reichmann *et al.*, each NKG2D half site consisted of a single cooperative module (unpublished data). Distance from the half-site cores may explain why the peripheral mutation N69W provides a fully additive gain observed in this study when combined with the sextuple mutant to make the septuple mutant [Fig. 2(B)]. However, factors other than distance must affect cooperativity, because two alterations in charge distribution at the interface at opposite ends of the NKG2D footprint, D15N and H158D, combine with negative additivity in the ND mutant [Fig. 2(B)].

Conclusion

Here, we demonstrate a rational, iterative enhancement of MICA that qualitatively changed NKG2D affinity from weak ($K_D = 2.5$ μM) to moderately tight ($K_D = 51$ nM) with seven mutations, engineering affinity past thresholds appropriate for applications such as immunoprecipitation and vaccination.[24,25] Different strategies of mutating residues that were at and below the binding interface enhanced affinity, although when combined, mutants often bound with partial or negative additivity. Three tests identified 32 out of 85 design scores as incorrect or destabilizing, with no wrongly identified scores for NKG2D-MICA, and with three wrongly identified scores combined for three other protein–protein interfaces. RosettaDesign scores could be compared with experimentally determined free energies, showing that simple design calculations with fixed backbone design can systematically enhance an existing protein interface.

Methods

Computational

RosettaDesign[26] v2.1 was used to model side chain mutations and calculate energies with the -fixbb -repack_neighbors -soft_rep options selected.[27,14] Structural coordinates from the PDB file (1HYR for NKG2D-MICA) were relaxed, repacked, and remodeled with Rosetta to provide wild-type models, which were then mutated, repacked, and evaluated. For each mutant, Rosetta calculated a score 100 times and an example with the lowest score from that set was used. Most scores converged two to nine times within the set of 100.

Experimental

Recombinant MICA and NKG2D proteins were produced and purified with affinity chromatography to $>\sim$95% purity and sized with size-exclusion chromatography using methods identical to those previously published in report of the first design strategy[7] to allow for comparison of results, including production of proteins by undergraduates in a biochemistry teaching laboratory.[28] Plasmids for expression of several mutant MICA molecules were constructed by Genscript (Piscataway, NJ).

SPR assays were also consistent with earlier work to allow for direct comparison of results, performed on a BIAcore 3000 and fit with a two-step model, which was supported by controls and biophysical tests.[7] We confirmed in Lengyel *et al*. that relative affinities on mutation for the MICA-NKG2D system are similar for a two-step kinetic model and a simple equilibrium model. (Recently, two-step modeling of SPR kinetic data has been validated biophysically for another protein–protein interface.[29]) The accuracy of our independent measurements can be assessed by comparing pairs of proteins with highly conservative mutations that were made and evaluated by different groups of students at different points in the project, giving identical results within error: e.g., wild-type vs. R64K ($\Delta\Delta G = -0.06 \pm 0.1$ kcal/mol); and R38T_H158D vs. R38T_H158D+Y157F ($\Delta\Delta G = -0.03 \pm 0.1$ kcal/mol). Kinetic data were gathered at five to nine temperatures and then combined into van't Hoff plots, with enthalpy calculated as reported in Lengyel *et al*.

Acknowledgments

We acknowledge the laboratory sections of BIO/CHM 4362 from 2008 to 2011, who expressed and purified many of these proteins. We thank Roland K. Strong for access to the BIAcore 3000 used for SPR measurements (Fred Hutchinson Cancer Research Center).

References

1. Kaufmann KW, Lemmon GH, DeLuca SL, Sheehan JH, Meiler J (2010) Practically useful: what the Rosetta protein modeling suite can do for you. Biochemistry 49: 2987–2998.
2. Pantazes RJ, Grisewood MJ, Maranas CD (2011) Recent advances in computational protein design. Curr Opin Struct Biol 21:467–472.
3. Karanicolas J, Kuhlman B (2009) Computational design of affinity and specificity at protein–protein interfaces. Curr Opin Struct Biol 19:458–463.
4. Mandell DJ, Kortemme T (2009) Computer-aided design of functional protein interactions. Nat Chem Biol 5:797–807.
5. Fleishman SJ, Whitehead TA, Strauch E-M, Corn JE, Qin S, Zhou H-X, Mitchell JC, Demerdash ONA,

Takeda-Shitaka M, Terashi G, Moal IH, Li X, Bates PA, Zacharias M, Park H, Ko J-S, LeeH, Seok C, Bourquard T, Bernauer J, Poupon A, Azé J, Soner S, Ovali ŞK, Ozbek P, Tal NB, Haliloglu T, Hwang H, Vreven T, Pierce BG, Weng Z, Pérez-Cano L, Pons C, Fernández-Recio J, Jiang F, Yang F, Gong X, Cao L, Xu X, Liu B, Wang P, Li C, Wang C, Robert CH, Guharoy M, Liu S, Huang Y, Li L, Guo D, Chen Y, Xiao Y, London N, Itzhaki Z, Schueler-Furman O, Inbar Y, Potapov V, Cohen M, Schreiber G, Tsuchiya Y, Kanamori E, Standley DM, Nakamura H, Kinoshita K, Driggers CM, Hall RG, Morgan JL, Hsu VL, Zhan J, Yang Y, Zhou Y, Kastritis PL, Bonvin AMJJ, Zhang W, Camacho CJ, Kilambi KP, Sircar A, Gray JJ, Ohue M, Uchikoga N, Matsuzaki Y, Ishida T, Akiyama Y, Khashan R, Bush S, Fouches D, Tropsha A, Esquivel-Rodríguez J, Kihara D, Stranges PB, Jacak R, Kuhlman B, Huang S-Y, Zou X, Wodak SJ, Janin J, Baker D (2011) Community-wide assessment of protein-interface modeling suggests improvements to design methodology. J Mol Biol 414: 289–302.

6. Azoitei ML, Correia BE, Ban Y-EA, Carrico C, Kalyuzhniy O, Chen L, Schroeter A, Huang P-S, McLellan JS, Kwong PD, Baker D, Strong RK, Schief WR (2011) Computation-guided backbone grafting of a discontinuous motif onto a protein scaffold. Science 334:373–376.
7. Lengyel CSE, Willis LJ, Mann P, Baker D, Kortemme T, Strong RK, McFarland BJ (2007) Mutations designed to destabilize the receptor-bound conformation increase MICA-NKG2D association rate and affinity. J Biol Chem 282:30658–30666.
8. Obeidy P, Sharland AF (2009) NKG2D and its ligands. Int J Biochem Cell Biol 41:2364–2367.
9. Kortemme T, Morozov AV, Baker D (2003) An orientation-dependent hydrogen bonding potential improves prediction of specificity and structure for proteins and protein–protein complexes. J Mol Biol 326:1239–1259.
10. Li P, Morris DL, Willcox BE, Steinle A, Spies T, Strong RK (2001) Complex structure of the activating immunoreceptor NKG2D and its MHC class I-like ligand MICA. Nat Immunol 2:443–451.
11. Mayer C, Snyder WK, Swietlicka M, VanSchoiack A, Austin C, McFarland B (2009) Size-exclusion chromatography can identify faster-associating protein complexes and evaluate design strategies. BMC Res Notes 2:135.
12. Lippow SM, Wittrup KD, Tidor B (2007) Computational design of antibody-affinity improvement beyond in vivo maturation. Nat Biotechnol 25:1171–1176.
13. Haidar JN, Pierce B, Yu Y, Tong W, Li M, Weng Z (2009) Structure-based design of a T-cell receptor leads to nearly 100-fold improvement in binding affinity for pepMHC. Proteins 74:948–960.
14. Sammond DW, Eletr ZM, Purbeck C, Kimple RJ, Siderovski DP, Kuhlman B (2007) Structure-based protocol for identifying mutations that enhance protein–protein binding affinities. J Mol Biol 371:1392–1404.
15. Keeble AH, Joachimiak LA, Maté MJ, Meenan N, Kirkpatrick N, Baker D, Kleanthous C (2008) Experimental and computational analyses of the energetic basis for dual recognition of immunity proteins by colicin endonucleases. J Mol Biol 379:745–759.
16. Bonsor DA, Postel S, Pierce BG, Wang N, Zhu P, Buonpane RA, Weng Z, Kranz DM, Sundberg EJ (2011) Molecular basis of a million-fold affinity maturation process in a protein–protein interaction. J Mol Biol 411:321–328.
17. Insaidoo FK, Borbulevych OY, Hossain M, Santhanagopolan SM, Baxter TK, Baker BM (2011) Loss of T cell antigen recognition arising from changes in peptide and major histocompatibility complex protein flexibility. J Biol Chem 286:40163–40173.
18. Wu Y, Gao F, Liu J, Qi J, Gostick E, Price DA, Gao GF (2011) Structural basis of diverse peptide accommodation by the Rhesus Macaque MHC class I molecule Mamu-B*17: insights into immune protection from Simian Immunodeficiency Virus. J Immunol 187: 6382–6392.
19. Reichmann D, Rahat O, Albeck S, Meged R, Dym O, Schreiber G (2005) The modular architecture of protein–protein binding interfaces. Proc Natl Acad Sci U S A 102:57–62.
20. Reichmann D, Cohen M, Abramovich R, Dym O, Lim D, Strynadka NC, Schreiber G (2007) Binding hot spots in the TEM1-BLIP interface in light of its modular architecture. J Mol Biol 365:663–679.
21. Pierce BG, Haidar JN, Yu Y, Weng Z (2010) Combinations of affinity-enhancing mutations in a T cell receptor reveal highly nonadditive effects within and between complementarity determining regions and chains. Biochemistry 49:7050–7059.
22. Muller BH, Savatier A, L'Hostis G, Costa N, Bossus M, Michel S, Ott C, Becquart L, Ruffion A, Stura EA, Ducancel F (2011) In vitro affinity maturation of an anti-PSA antibody for prostate cancer diagnostic assay. J Mol Biol 414:545–562.
23. Poulsen TR, Jensen A, Haurum JS, Andersen PS (2011) Limits for antibody affinity maturation and repertoire diversification in hypervaccinated humans. J Immunol 187:4229–4235.
24. Dyson MR, Zheng Y, Zhang C, Colwill K, Pershad K, Kay BK, Pawson T, McCafferty J (2011) Mapping protein interactions by combining antibody affinity maturation and mass spectrometry. Anal Biochem 417: 25–35.
25. Stanfield RL, Julien J-P, Pejchal R, Gach JS, Zwick MB, Wilson IA (2011) Structure-based design of a protein immunogen that displays an HIV-1 gp41 neutralizing epitope. J Mol Biol 414:460–476.
26. Rohl CA, Strauss CEM, Misura KMS, Baker D (2004) Protein structure prediction using Rosetta. In: Ludwig B, Michael LJ, Eds. Methods in enzymology. Academic Press (San Diego, CA), 383:66–93.
27. Dantas G, Corrent C, Reichow SL, Havranek JJ, Eletr ZM, Isern NG, Kuhlman B, Varani G, Merritt EA, Baker D (2007) High-resolution structural and thermodynamic analysis of extreme stabilization of human procarboxypeptidase by computational protein design. J Mol Biol 366:1209–1221.
28. Peterson MJ, Snyder WK, Westerman S, McFarland BJ (2011) Preparative protein production from inclusion bodies and crystallization: a seven-week biochemistry sequence. J Chem Educ 88:986–989.
29. Anunciado D, Dhar A, Gruebele M, Baranger AM (2011) Multistep kinetics of the U1A–SL2 RNA complex dissociation. J Mol Biol 408:896–908.